JOURNAL OF Materials CHEMISTRY

Intermediates in the formation of microporous layered tin(IV) sulfide materials†

Tong Jiang,[a] Alan Lough,[a] Geoffrey A. Ozin*[a] and Robert L. Bedard[b]

[a]*Materials Chemistry Research Group, Lash Miller Chemical Laboratories, University of Toronto, Toronto, Ontario, Canada, M5S 3H6*

[b]*UOP Research and Development, 50 E. Algonquin Rd., Des Plaines, Illinois, 60017-5017, USA*

The formation pathway of microporous layered tin(IV) sulfides $A_2Sn_3S_7$ and $A_2Sn_4S_9$ (A = cation), respectively denoted SnS-1 and SnS-3, synthesized from elemental Sn and S sources in the presence of templates and mineralizers has been studied. Three types of reaction intermediates, dimeric $[Sn_2S_6]^{4-}$, polysulfides $[Sn(S_4)_3]^{2-}$/$[Sn(S_4)_2(S_6)]^{2-}$ and thiosulfate $[S_2O_3]^{2-}$, have been isolated and characterized by single crystal X-ray diffraction structure analysis. UV–VIS and ^{119}Sn NMR studies of mother-liquors of representative SnS-*n* systems indicate that the dimeric $[Sn_2S_6]^{4-}$ anion is the predominant solution tin-containing species and a likely basic building unit for the SnS-*n* frameworks. The role of template cations has also been examined. The pH dependent condensation–polymerization of the dimeric $[Sn_2S_6]^{4-}$ precursor in the presence of template cations is believed to be responsible for the formation of the SnS-*n* structures. The dissolution and redox reactions of the elemental Sn metal and S_8 powders are found to be extremely sensitive to pH, mineralizers and temperature. Reagents, such as sulfide, fluoride, hydroxide and amines that can react with tin, sulfur and various tin sulfide and polysulfide intermediates are good mineralizers. To produce large single crystals of the SnS-*n* materials, the concentration and strength of mineralizers need to be kept low, however, to prepare phase pure materials, the presence of excess mineralizer is required. In general, amine templates are strong mineralizers for tin metal particles, presumably through coordination to various tin polysulfide and sulfide intermediates. As a result, amine templates/mineralizers provide cleaner and smaller product crystals under reaction conditions that are similar to those used with tetraalkylammonium hydroxide templates. Surprisingly, it was found that $(DABCOH)_2Sn_3S_7$, denoted DABCOH-SnS-1, can be formed using 'very soft chemistry' at room temperature and atmospheric pressure conditions, from an aqueous solution of $[Sn_2S_6]^{4-}$ simply by the precise control of pH. The hydrothermal reaction conditions that are generally employed in the synthesis of SnS-*n* materials only serve to digest the starting material.

We have sucessfully synthesized two new families of tin(IV) sulfide-based materials, $A_2Sn_3S_7$ and $A_2Sn_4S_9$ (A = cation), denoted SnS-1 and SnS-3, under hydrothermal reaction conditions by utilizing elemental Sn and S as source materials and amines or quaternary alkylammonium hydroxides as templates and mineralizers.[1] Their microporous layered structures were established by single crystal X-ray diffraction (SCXRD) structure analysis. The tin sulfide layer of the SnS-1 structure type contains hexagonally shaped 24-atom rings which are constituted by six Sn_3S_4 broken-cube cluster building units, linked together by double bridge Sn(μ-S)$_2$Sn sulfur bonds. The SnS-3 structure type contains elliptically shaped 32-atom rings which are also constructed from six Sn_3S_4 broken-cube clusters. However, they are linked by double bridge Sn(μ-S)$_2$Sn sulfur bonds as well as tetrahedral edge-bridging (μ-S_2SnS_2) spacer units.

The SnS-1 structure has been formed in the presence of a wide range of template cations, such as Me_4N^+, Et_4N^+, $QUINH^+$ (quinuclidinium), $DABCOH^+$ (protonated 1,8-diazabicyclooctane), and a mixed template system of NH_4^+/Et_4N^+, while the SnS-3 structure resulted from the use of $Pr^n{}_4N^+$ and $Bu^n{}_4N^+$. We have also investigated the reaction conditions that play an important role in the formation of these materials, such as aging, agitation and the reaction profile. One interesting question is how the microporous tin sulfide layers evolve from the elemental Sn/S sources under hydrothermal reaction conditions? What are the functions of the organics? How do crystallization conditions, such as pH, mineralizers, agitation, and temperature, affect the nucleation and crystal growth of the final product? Can one synthesize these materials through building block assembly at room temperature? All of these questions are related to a contemporary aspect of solid state synthesis, namely, the rational design or crystal engineering of functional solid state materials.[2,3] We have been interested in the connections between synthesis–structure–property–function of metal sulfide-based microporous materials for several years. Various transition metal gemanium sulfide open-framework materials have been synthesized through a modular-assembly approach using the adamantanoid $[Ge_4S_{10}]^{4-}$ cluster and transition metal M^{2+}/M^+ cations as precursors.[4] Recently, we have demonstrated that the microporous layered structures of SnS-*n* materials can also be formed through the self-assembly of $[Sn_2S_6]^{4-}$ dimers.[5]

Here, we report the details of the formation and crystallization of SnS-*n* materials from elemental Sn and S sources in the presence of mineralizers and templates. Reaction intermediates and their chemistry are examined using solution phase ^{119}Sn NMR and UV–VIS spectroscopy, powder and single crystal XRD analysis. The structure of three types of molecular tin(IV) sulfide intermediates are described. A possible pathway for the mode of formation of the SnS-*n* materials is proposed. The role of template, mineralizers, reaction profiles and pH are also examined. A 'very soft chemistry' preparation of the SnS-1 materials at room temperature and atmospheric pressure, through the pH dependent assembly of dimer building blocks in an aqueous solution is demonstrated for the first time.

Dimeric $[Sn_2S_6]^{4-}$ building block: investigation of the mother-liquors

The mother-liquors of TEA-SnS-1 and TPA-SnS-3 were investigated as representative systems for the SnS-1 and SnS-3 families, respectively. The starting reaction mixtures

† Additional characterisation data (**SUP 537331**; 7 pp.) deposited with the British Library. Details are available from the editorial office.

TEAOH/Sn/2S : 30 H_2O and TPAOH : Sn : 2.25 S : 160 H_2O were crystallized at 150 °C over a period of 1–10 days. The resulting solid products were confirmed to be TEA-SnS-1 and TPA-SnS-3 by PXRD. Depending on the crystallization conditions, unreacted tin metal may be present in the final solid product. The resulting mother-liquors were investigated by solution phase ^{119}Sn NMR and UV–VIS spectroscopy. In both cases, one predominant ^{119}Sn NMR signal, together with two satellite peaks were observed with a chemical shift of δ 57–60 (relative to Me_4Sn). The ratio of the intensities of the main peak to that of the satellites is estimated to be *ca.* 10–12, close to the value of 10.9 expected for a dimeric tin compound.[6] The satellite peaks arise from the ^{117}Sn–^{119}Sn and ^{115}Sn–^{119}Sn nuclear spin-spin couplings (these three isotopes all have a spin of 1/2 with a natural abundance of 8.58% for ^{119}Sn, 7.68% for ^{117}Sn, and 0.36% for ^{115}Sn). An aqueous solution of dimeric $(CHAH)_4Sn_2S_6$ displays a ^{119}Sn NMR chemical shift signal at δ 59. The low sensitivity of ^{119}Sn NMR, 0.052 relative to an equal number of ^{1}H, together with the poor solubility of $(CHAH)_4Sn_2S_6$ in water and common organic solvents, are responsible for the observed low signal/noise ratio. The NMR chemical shift of ^{119}Sn is known to be extremely sensitive to, for example, oxidation state, ligand type and coordination number, and covers a wide range of up to 2700 ppm.[1c,7,8] For instance, the chemical shift for tetrahedral tin(IV) in solid Na_4SnS_4 occurs at δ 68,[7] distorted trigonal-bipyramidal tin(IV) in SnS-1 materials at δ −344,[1c] octahedral tin(IV) in berndtite SnS_2 at δ −765,[7] and octahedral tin(IV) in SnO_2 at δ −603 (relative to Me_4Sn). The weak ^{119}Sn NMR signal observed at around δ 82 is best assigned to a tetrahedral tin(IV) sulfide species, most likely the monomeric SnS_4^{4-} anion.

The ^{119}Sn NMR data indicate that the dimeric $[Sn_2S_6]^{4-}$ anion is present as the dominant tin species in the mother-liquors of SnS-1 and SnS-3 preparations. This receives additional support from UV–VIS spectroscopic investigations of mother-liquors of TEA-SnS-1 and TPA-SnS-3 as well as the $(CHAH)_4Sn_2S_6$ dimer. The diagnostic band at 270 nm was used to determine the absorption coefficient of the $(CHAH)_4Sn_2S_6$ dimer in aqueous solution. The calculated value was found to be 2×10^4 dm^3 mol^{-1} cm^{-1} which indicates that the 270 nm band is best assigned to a S^{-II} to Sn^{IV} ligand-to-metal charge-transfer (LMCT) electronic transition. Assuming that the absorption coefficient remains unchanged for the dimers in the mother-liquors of an SnS-1 and SnS-3 hydrothermal synthesis, one can estimate the concentration of $[Sn_2S_6]^{4-}$ in solution. For representative TPA-SnS-3 mother-liquors, a typical concentration of the dimer was found to be between 2×10^{-2} and 6×10^{-3} M and decreased when the reaction time was extended from 1 to 10 days. When the tin content of the $[Sn_2S_6]^{4-}$ in the mother-liquors was taken together with the quantity of tin in the solid phase product of TPA-SnS-3, one can essentially account for the entire mass of elemental tin used in the actual synthesis of TPA-SnS-3. The quantity of unreacted tin in the solid product was determined through a quantitative PXRD analysis.

$(CHAH)_4Sn_2S_6$ isolation and structure determination

It has also proven possible to isolate $(CHAH)_4Sn_2S_6$ from the mother-liquors of the Sn/S-based synthesis in the CHA template system and establish its structure by single crystal (SC)XRD analysis. The single crystal data of $(CHAH)_4Sn_2S_6$ are listed in Table 1. $(CHAH)_4Sn_2S_6$ contains the $[Sn_2S_6]^{4-}$ dimer, the structure of which is based on two edge-sharing tetrahedral SnS_4 units, Fig. 1A. The $[Sn_2S_6]^{4-}$ dimer moiety is surrounded by the $CHAH^+$ cations. The structure analysis of $(CHAH)_4Sn_2S_6$ establishes that the cyclohexylamine is protonated on the nitrogen of the primary amine ($CHAH^+$) and that hydrogen-bonding between the $CHAH^+$ protons and the terminal and bridging sulfurs of the $[Sn_2S_6]^{4-}$ dimer creates an extended network structure, an illustration of part of which is shown in Fig. 1A. Note that the $(Me_4N)_4Sn_2S_6$ dimer has also been crystallized from the mother-liquor of a TMA-SnS-1 hydrothermal synthesis. The Me_4N^+ cations are found to locate in close proximity to the negatively charged terminal sulfurs of the $[Sn_2S_6]^{4-}$ dimer.[9]

Formation of the SnS-*n* structure from the $[Sn_2S_6]^{4-}$ dimer

All of the above information suggests that the $[Sn_2S_6]^{4-}$ dimer species is a likely precursor for the formation of microporous

Table 1 Summary of crystal data and least-squares refinement parameters

compound	$(CHAH)_4Sn_2S_6$ **1**	$(DABCOH)_2Sn(S_4)_3$/ $(DABCOH)_2Sn(S_4)_2(S_6)$ **2**	$(AMTAH)_2S_2O_3$ **3**
empirical formula	$C_{24}H_{56}N_4S_6Sn_2$	$C_{12}H_{26}N_4S_{13}Sn$	$C_{20}H_{36}N_2O_3S_2$
M_r	840.47	761.84	416.63
crystal system	monoclinic	orthorhombic	monoclinic
space group	*C*2/*c*	*Pbca*	$P\bar{1}$
a/Å	26.861(5)	10.493(2)	6.461(3)
b/Å	7.466(1)	18.965(4)	6.574(2)
c/Å	20.109(4)	27.251(5)	27.777(9)
V/Å^3	4032.744	5422.942	1179.817
α/°	90	90	90.64(3)
β/°	111.14(3)	90	90.68(3)
γ/°	90	90	118.21(3)
Z	4	8	2
temperature/K	293	293	213
D_c/g cm^{-3}	1.467	1.866	1.331
μ(Mo-Kα)/cm^{-1}	16.80	19.56	13.31
diffractometer	Enraf-Nonius CAD4	Enraf-Nonius CAD4	Siemens P4
F(000)	1696	3072	452
ω scan width, °	0.80 + 0.35 tan θ	0.80 + 0.35 tan θ	0.76
range θ collected, °	1.63–22.49	1.49–22.48	3.52–27.00
independent reflections	1672	3544	4474
$R1^a$ [$I > 2\sigma(I)$]	0.0326	0.0561	0.0937
$wR2^b$ (all data)	0.0904	0.3979	0.3868
goodness of fit	1.109	1.062	1.089
maximum peak in final ΔF map, e/Å^{-3}	0.369	0.992	0.866

$^aR1 = \Sigma(F_o - F_c)/\Sigma(F_o)$. $^bwR2 = [\Sigma[w(F_o^2 - F_c^2)^2]/\Sigma[w(F_o^2)^2]]^{1/2}$.

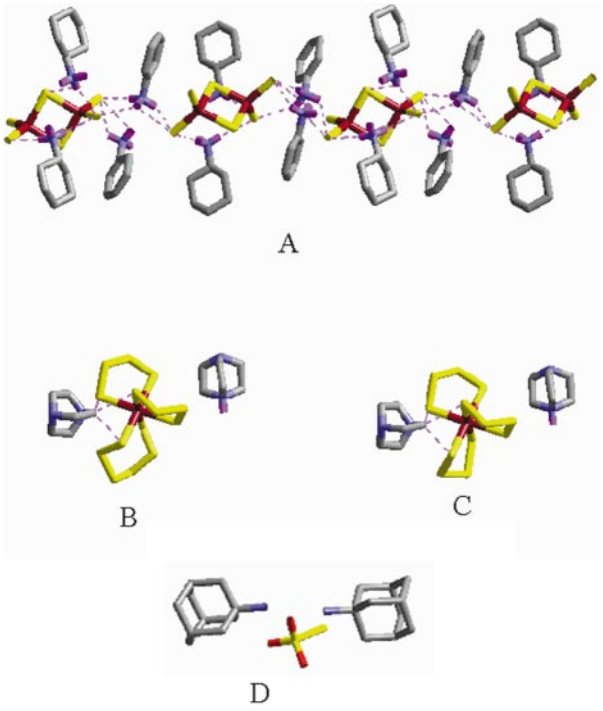

Fig. 1 Single crystal XRD structures of the molecular reaction intermediates in the formation of SnS-*n* materials (A) $(CHAH)_4Sn_2S_6$, (B) $(DABCOH)_2Sn(S_4)_2(S_6)$, (C) $(DABCOH)_2Sn(S_4)_3$ and (D) $(AMTAH)_2S_2O_3$

layered R-SnS-*n* materials. If this is correct, then it should be possible to prepare the SnS-*n* materials directly from a $[Sn_2S_6]^{4-}$ dimer source. This has proven to be possible in a study on the synthesis of DABCOH-SnS-1 from a mixture of $DABCO:Sn:2\,S:(NH_4)_2S:30\,H_2O$, dynamically in a tumbling reactor. The mother-liquor that resulted from a crystallization period of 3 h at 150 °C contains dimer $[Sn_2S_6]^{4-}$ as the dominant tin-containing species as only a single broad signal at δ 56.5 was observed in its solution phase ^{119}Sn NMR spectrum. The UV–VIS spectrum also displays the diagnostic absorption band for the $[Sn_2S_6]^{4-}$ dimer at 270 nm. The corresponding solid phase product was highly crystalline DABCOH-SnS-1, without any detectable amorphous or crystalline impurities, as confirmed by PXRD, Fig. 2A, and Mössbauer measurements.[1c]

Interestingly, at room temperature, an off-white solid was observed to precipitate slowly from a clear mother-liquor which was stored in a vial at room temperature. The phase identity of this solid, as determined by PXRD, Fig. 2C, was DABCOH-SnS-1. At room temperature and atmospheric pressure, the dimeric $[Sn_2S_6]^{4-}$ species slowly condenses to the microporous layered framework of DABCOH-SnS-1. Moreover, this association reaction was found to be sensitive to the type of atmosphere in the vial. The same mother-liquor collected and sealed under N_2 with a pH of about 10 remained as a clear solution for weeks at room temperature, however, in air it gave rise to DABCOH-SnS-1 solid within a couple of hours. Bubbling CO_2 into the mother-liquor under N_2 dramatically accelerates the assembly of $[Sn_2S_6]^{4-}$ to DABCOH-SnS-1 causing it to occur within a couple of minutes, meanwhile the pH of the mother-liquor was found to have dropped to 9.4 at the end of the reaction. The PXRD pattern of the resulting solid product of DABCOH-SnS-1 is shown in Fig. 2B. Note that an extension of the crystallization time from 3 h to 4 days at 150 °C did not increase the yield of the DABCOH-SnS-1 product, which was found to be between 60–70%. This suggests that the assembly of the dimer to the SnS-1 framework is pH dependent and reaches an equilibrium value at a given pH.

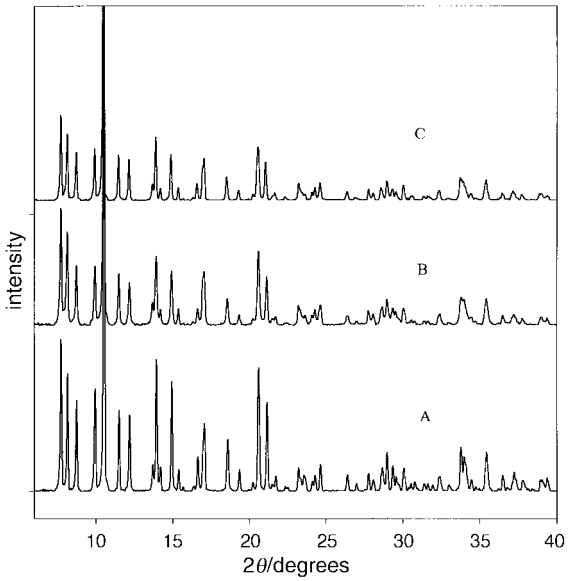

Fig. 2 The PXRD patterns of the solid products crystallized from (A) a mixture of $DABCO:Sn:2\,S:(NH_4)_2S:30\,H_2O$ at 150 °C for 3 hours, (B) the mother-liquor of (A) collected under N_2 and exposed to a stream of CO_2 for 10 min, and (C) the mother-liquor of (A) stored at room temperature in a loosely capped vial in air for 5 days

It is interesting that the Sn_3S_4 broken cube clusters that constitute the microporous layered structures of both R-SnS-1 and R-SnS-3 can be visualized in terms of the assembly and linkage of two dimer units in the arrangement illustrated in Fig. 3. Presumably, some of the terminal sulfurs of the dimer are protonated under the conditions of a hydrothermal

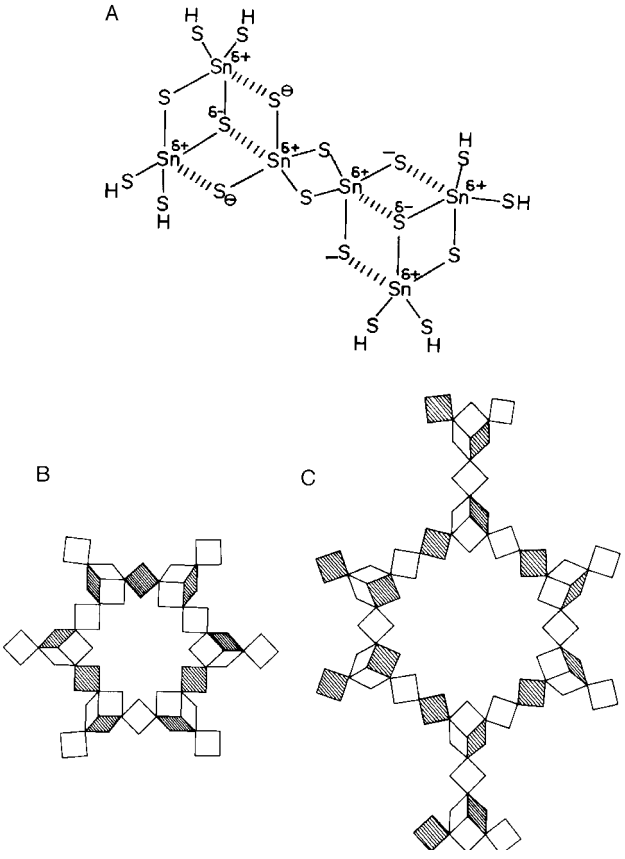

Fig. 3 Illustration of (A) the assembly of $[Sn_2S_6]^{4-}$ building blocks to the Sn_3S_4 broken cube cluster sub-units, (B, C) the R-SnS-1 and R-SnS-3 structural motifs obtained from the assembly of $[Sn_2S_6]^{4-}$ building blocks

synthesis, and in the presence of the template are linked through a condensation–polymerization reaction involving tin(IV) hydrosulfide groups. This would explain the observed pH-dependent aggregation of the dimer. At a given pH, an equilibrium between the dimer $[Sn_2S_6]^{4-}$ and its conjugate acids $[Sn_2S_6H_x]^{4-x}$ ($x=0$–4) is expected to exist, which can be shifted to the acid side by a reduction of pH. This implies that more protonated $[Sn_2S_6H_x]^{4-x}$ would be generated at lower pH and their condensation–polymerization will lead to the formation of the SnS-1 framework. Note that evidence for what is most likely the initial step in this condensation–polymerization process has recently been obtained through the isolation and SCXRD structure determination of a chalcogenide bridged dimer-of-dimers, $[Sn_2Se_5(\mu\text{-}Se)Sn_2Se_5]^{6-}$ species.[10]

In addition, the nature of the final products should also be rather sensitive to pH. In fact, the degree of condensation is expected to increase at lower pH conditions.[11] Indeed, it was found that on reducing the initial pH of a TPA-SnS-3 reaction mixture from 13–14 to 10 by addition of an aqueous HCl solution to the aforementioned reaction mixture, one observes by PXRD the formation of the dense packed berndtite, SnS_2, layer phase. By contrast, on changing the initial pH to 12.2, PXRD shows that a new layered material with an interlamellar spacing of 10.24 Å is produced with some unreacted tin. It is clear from the above results that the pH of the reaction mixture plays a crucial role in the assembly of the $[Sn_2S_6]^{4-}$ building blocks and the formation of the SnS-*n* materials.

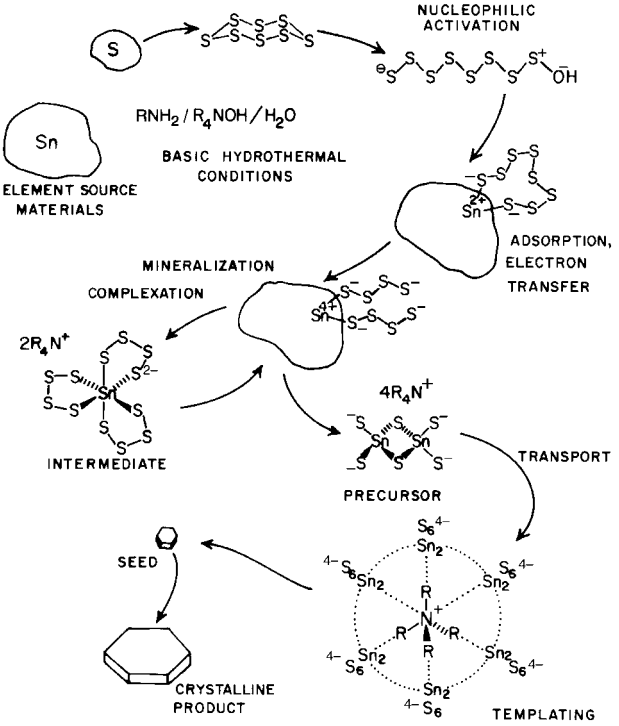

Fig. 4 Overall scheme illustrating the mode of formation of the SnS-*n* microporous layered tin(IV) sulfides, from redox mineralization of elemental Sn and S under hydrothermal basic reaction conditions in the presence of an organic template

Redox-assisted mineralization

As demonstrated above the dimeric $[Sn_2S_6]^{4-}$ species appears to be the precursor for the formation of the microporous layered DABCOH-SnS-1 material. Protonation and condensation–polymerization of $[Sn_2S_6]^{4-}$ forms the SnS-1 and SnS-3 materials. The next question concerns how the $[Sn_2S_6]^{4-}$ dimer species is formed under the hydrothermal reaction conditions from elemental tin and sulfur in the presence of templates? Based on literature precedents, elemental sulfur (S_8) can be activated by ring-opening nucleophilic attack by a base, such as an amine or hydroxide, eqn. (1):[12]

$$S_8 + RNH_2 \rightarrow {}^{-}S{-}S_6{-}S{-}{}^{+}NH_2R \qquad (1)$$

In addition, donor molecules like amines are able to promote reactions between powdered sulfur (S_8) and a large variety of metal particles, such as Cu, Zn, Mn, Fe, Ni, through coordinating to metal polysulfide intermediates.[13–15] The amine facilitates the redox reaction between the metal and sulfur by stabilizing and solubilizing the metal polysulfide intermediates. One can surmise that under the hydrothermal reaction conditions used for the synthesis of the SnS-*n* materials the cyclooctasulfur molecule is either activated by nucleophilic amine, hydroxide or through adsorption at electron-rich tin sites present in the surface of the elemental tin particles. Sulfur can also react readily with sulfide to form soluble polysulfides.[16] This working hypothesis makes it possible to understand the chemistry occurring in the Sn/S hydrothermal synthesis of R-SnS-*n* materials, in terms of a redox assisted mineralization process, as illustrated in Fig. 4. Cleavage of sulfur–sulfur bonds can be envisaged to occur through a series of tin to sulfur electron transfer reactions, involving oxidative addition of surface tin atoms into a sulfur–sulfur bond of S_8. This reaction serves to solubilize elemental tin and sulfur reagents, proceeding through intermediate stages such as those listed in eqn. (2)–(8), to yield various tin(IV) polysulfide and sulfide complexes that are believed to participate in the formation of R-SnS-*n* materials. Amine molecules and hydroxide presumably stabilize and solubilize the intermediates *via* coordination to the tin center.

$$Sn + S_8 \rightarrow Sn^{2+} + S_8^{2-} \qquad (2)$$

$$Sn^{2+} + S_8^{2-} \rightarrow Sn^{4+} + S_6^{2-} + S_2^{2-} \qquad (3)$$

$$Sn^{2+} + S_8^{2-} \rightarrow Sn^{4+} + 2S_4^{2-} \qquad (4)$$

$$Sn^{4+} + 3S_4^{2-} \rightarrow [Sn(S_4)_3]^{2-} \qquad (5)$$

$$Sn^{4+} + 2S_4^{2-} + S_6^{2-} \rightarrow [Sn(S_4)_2S_6]^{2-} \qquad (6)$$

$$Sn + S_2^{2-} \rightarrow Sn^{2+} + 2S^{2-} \qquad (7)$$

$$2Sn^{4+} + 6S^{2-} \rightarrow [Sn_2S_6]^{4-} \qquad (8)$$

$(DABCOH)_2Sn(S_4)_3$ and $(DABCOH)_2Sn(S_4)_2(S_6)$ isolation and structure determination

It has proven possible to isolate tin(IV) polysulfide intermediates, $[Sn(S_4)_3]^{2-}$ and $[Sn(S_6)(S_4)_2]^{2-}$, from a reaction mixture of $DABCO:Sn:2S:35H_2O$ crystallized at a reduced temperature of 100 °C. The single crystal data for $(DABCOH)_2[Sn(S_4)_3]$ and $(DABCOH)_2[Sn(S_4)_2(S_6)]$ are listed in Table 1. The unit cell was found to contain an equimolar mixture of six-coordinate quasi-octahedral tin(IV) polysulfide complexes determined to be $[Sn(S_4)_3]^{2-}$ and $[Sn(S_6)(S_4)_2]^{2-}$, where the charge-balancing cations were established to be singly protonated $DABCOH^+$, hydrogen-bonded to the sulfurs of the polysulfide ligands, Fig. 1B, C. The former contains three bidentate tetrasulfide ligands, while the latter has one bidentate hexasulfide and two bidentate tetrasulfide ligands. Note that the single crystal structure of $(Et_4N)_2[Sn(S_4)_3]_{0.4}[Sn(S_4)_2(S)_6]_{0.6}$ has been reported,[17] in which $[Sn(S_4)_3]^{2-}$ and $[Sn(S_6)(S_4)_2]^{2-}$ were found to co-exist in a ratio of 4 : 6.

$(AMTAH)_2S_2O_3$ isolation and structure determination

As described earlier, the assembly of the dimer building blocks in the presence of organic templates is a likely pathway for the formation of the microporous layered R-SnS-*n* materials, Fig. 3. Based on the redox reactions described above, the ratio of S^{2-}/Sn^{4+} produced in the reaction mixture is limited to 2, which is smaller than that found in either of the solid products R-SnS-1 and R-SnS-3, that is, 2.33 : 1 and 2.25 : 1 respectively, or of the dominant solution tin sulfide species $[Sn_2S_6]^{4-}$, that is 3 : 1. In order to maintain charge balance in the systems which do not contain extra amounts of the S^{2-} source in the starting reaction mixture, one has to invoke the contribution of some kind of base-induced redox disproportionation of the S_8 to, for example, sulfide and sulfate/thiosulfate, eqn. (9) and (10):[16]

$$1/2S_8 + 12H_2O \rightarrow 3S^{2-} + SO_4{}^{2-} + 8H_3O^+ \quad (9)$$

$$1/2S_8 + 9H_2O \rightarrow 2S^{2-} + S_2O_3{}^{2-} + 6H_3O^+ \quad (10)$$

A white precipitate was observed when a solution of $BaCl_2$ was introduced to the mother-liquors of TEA-SnS-1 and TPA-SnS-3 obtained from $TEAOH : Sn : 2\,S : 30\,H_2O$ and $TPAOH : Sn : 2.25\,S : 160\,H_2O$ as described above. This indicates the presence of either sulfate and/or thiosulfate anions in the mother-liquors. The standard tests for sulfide and thiosulfate, for example, $HgCl_2$ and $[Fe(CN)_5(NO)]^{2-}$,[18] show interference from $[Sn_2S_6]^{4-}$. Nevertheless, single crystals of 1-adamantanammonium thiosulfate have been crystallized from a reaction mixture of $2\,AMTA : Sn : 2.33\,S : 100\,H_2O$ and characterized by SCXRD analysis.[19] The temperature profile involved slow heating of the reaction mixture to 150 °C in 10 h, holding at 150 °C for 13.5 h, and slow cooling to room temperature within 24 h. The single crystal data of $(AMTAH)_2S_2O_3$ is listed in Table 1 and the structure is shown in Fig. 1D. This existence of $(AMTAH)_2S_2O_3$ proves that the disproportionation of sulfur under these kinds of hydrothermal reaction conditions can occur. The co-formation of protons with the sulfate or thiosulfate anions as described in eqn. (9) and (10) is believed to be responsible for the observed pH drop of *ca.* 4–5 units during the hydrothermal synthesis of TEA-SnS-1 and TPA-SnS-3 materials from the aforementioned starting mixtures. It is worth noting that unreacted elemental sulfur can only be found in a reaction mixture with a low initial pH.

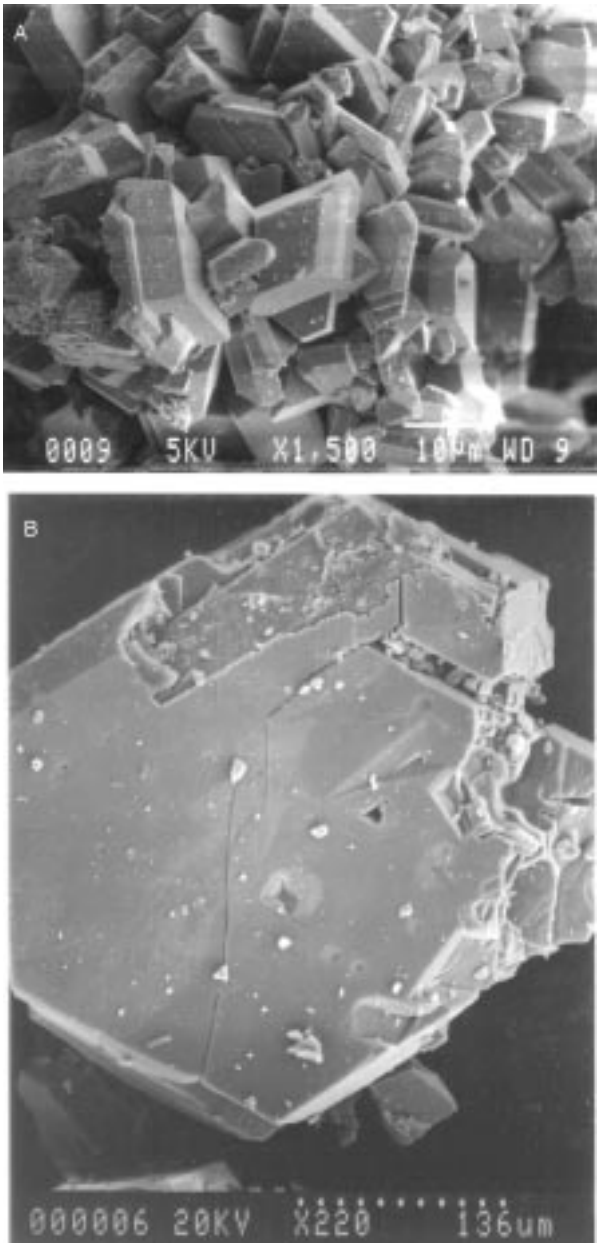

Fig. 5 A comparison of crystal sizes of (A) DABCOH-SnS-1, obtained from $DABCO : Sn : 2\,S : 30\,H_2O$ and (B) TEA-SnS-1, from $TEAOH : Sn : 2S : 30\,H_2O$, both were crystallized statically at 150 °C for 3 days

Discussion

Effect of template identity and concentration on the crystallization of SnS-*n* materials

In the course of this study it was found that under similar reaction conditions, SnS-*n* products obtained from an amine templated system tend to have a smaller crystal size and less unreacted tin, compared with those obtained from quaternary alkylammonium hydroxides. For example, under static crystallization conditions at 150 °C, single crystals of TEA-SnS-1 of a couple of hundred μm in size, accompanied by a large quantity of unreacted tin metal were obtained from a reaction mixture of $TEAOH : Sn : 2\,S : 30\,H_2O$, while crystals of DABCOH-SnS-1 of *ca.* 10 μm in size were formed from $DABCO : Sn : 2\,S : 30\,H_2O$ with a small quantity of unreacted tin. A comparison of the crystal size of TEA-SnS-1 and DABCOH-SnS-1 is shown in Fig. 5. This difference is believed to be attributed to the strong donor ability of the DABCO molecules. Presumably, amine molecules coordinate to the Sn(II,IV) site(s) in sulfide and polysulfide intermediates and help transport them away from the tin particle surface thereby exposing fresh tin surface sites for further reactions, Fig. 4. This process suppresses the passivation occurring on the tin particle surface and allows a more complete reaction of the tin metal particle. Furthermore, this process accelerates the redox reactions between Sn and S and the formation of the $[Sn_2S_6]^{4-}$ precursors. Consequently, more viable nuclei are formed at the initial nucleation step during the crystallization process. In the subsequent crystal growth step, they compete with one another for the supply of nutrients and consequently grow to smaller crystallite sizes.

For similar reasons, the size of crystallites obtained from the same amine template is expected to be dependent on the concentration of amine molecules. Larger crystals are anticipated from a starting reaction mixture containing a lower concentration of amine, and *vice versa*. Indeed, this trend has been observed and successfully exploited for growing large single crystals of DABCOH-SnS-1. On reducing the molar content x of DABCO from 2.5 to 0.2 in a starting reaction mixture of $x\,DABCO : Sn : 2\,S : (NH_4)_2S : 60\,H_2O$, the DABCOH-SnS-1 crystals were found to increase from several μm to *ca.* 1 mm in size, meanwhile the amount of unreacted tin increased from undetectable levels by PXRD and Mössbauer spectroscopy, to a primary solid phase. At low

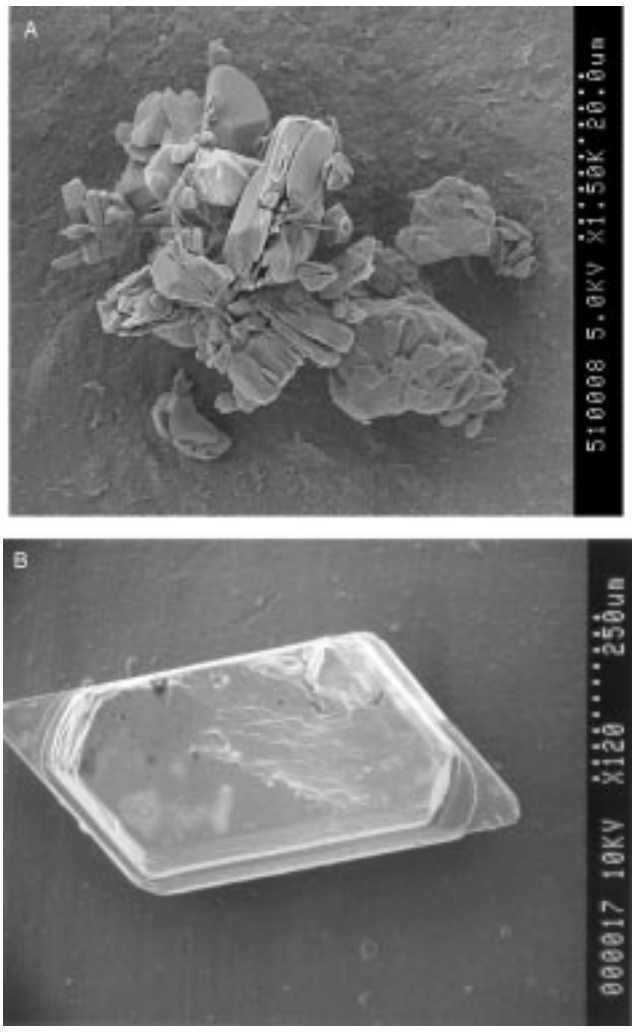

Fig. 6 A comparison of crystal sizes of DABCOH-SnS-1 crystallized from x DABCO : 2 $(NH_4)_2S$: Sn : 2S : 60 H_2O at 150 °C statically for 2 days, $x = 2$ (A) and 0.2 (B)

concentrations of DABCO, the DABCOH-SnS-1 crystals can be clearly seen as having crystallized and attached to the surface of tin particles, which is considered to be evidence for passivation. A comparison of the DABCOH-SnS-1 crystal sizes obtained from $x = 0.2$ and 2 in the above starting reaction mixture is shown in the SEM images of Fig. 6.

Templating role of the organic cations

The role of template agents in the hydrothermal synthesis of microporous materials, such as zeolites and aluminophosphates has been studied quite extensively.[20–22] In the crystallization of the SnS-*n* materials, the organic template is presumably involved in the organization and polymerization of the dimer species through coulombic, hydrogen-bonding and van der Waals interactions with the dimer, protonated dimer and other polymeric tin sulfide intermediates. The polymerization and nucleation of tin sulfides around the template cations is believed to be responsible for the formation of the microporous layered structures of SnS-1 and SnS-3 materials. This is consistent with the observation that small cations, such as Me_4N^+, Et_4N^+, QUINH$^+$ and DABCOH$^+$ result in the SnS-1 structure with smaller void spaces within and between the layers in comparison with the SnS-3 structure which is formed in the presence of larger cations $Pr^n{}_4N^+$ and $Bu^n{}_4N^+$. Furthermore, the size of the void spaces among various SnS-1 structures was found to bear a certain correspondence with the size of the template cations.[1c] It was also found that no crystalline product was formed when the organic cations were completely replaced by the small NH_4^+ cation in the starting reaction mixture. Interestingly, Cs-SnS-1 ($Cs_2Sn_3S_7 \cdot 0.5S_8$) was recently prepared through molten-salt synthesis at temperatures between 400 and 500 °C from a mixture of Sn, Cs_2S and S.[23] It is intriguing that S_8 is located in the 24-atom rings, and cannot be removed chemically or thermally without affecting the integrity of the tin sulfide framework. At high temperatures the occluded S_8 reacts with the SnS-1 framework and Cs^+ cation to form other tin sulfide phases. Clearly, the S_8 molecule interacts strongly with the tin sulfide framework and presumably functions as a template during the crystallization and formation of the Cs-SnS-1 structure. Note that a great deal of effort has been devoted to the synthesis of Cs-SnS-1 in the absence of elemental sulfur from SnS_2 source material, however, only a $Cs_2Sn_2S_6$ dimer was generated and structurally characterized by SCXRD.[24] It seems that the Cs^+ cation alone is too small to facilitate the organization and polymerization of the $[Sn_2S_6]^{4-}$-dimer to yield a microporous SnS-1 structure. However, Cs-SnSe-1 which is isostructural with the hypothetical Cs-SnS-1, had been prepared from Cs_2CO_3, $SnSe_2$, and SnSe through methanolothermal synthesis.[25] In view of the slightly larger 24-ring and the significantly larger interlamellar spacing in Cs-SnSe-1, the formation of Cs-SnSe-1 in methanol seems to be attributed to solvation by methanol. The hydrophobic methyl groups in $Cs(MeOH)_x^+$ may interact sufficiently with hydrophobic tin selenide intermediates to be able to direct the formation of Cs-SnSe-1.

Real-time *in situ* energy-dispersive synchrotron X-ray diffraction has been used to monitor the hydrothermal synthesis of TMA-SnS-1 from a reaction mixture of Sn : 2.2 S : TMAOH : 35 H_2O at 175 °C.[26] The TMA-SnS-1 has the orthorhombic space group $P2_12_12_1$, in which the tin sulfide microporous layers are parallel to the (001) plane.[1,5,19,24] It was found that the X-ray reflection corresponding to the interlamellar distance, d_{200}, emerged first and after a short crystallization time of 10 min. This was followed by a slow growth of *hk*0 and *hkl* reflections which are related to ordering within the layers and registry of adjacent lamellae, respectively. To amplify, the growth of the 111 reflection was continuing after 62 h of reaction, while the 002 peak reached its maximum within 10 h. This suggests that the $[Sn_2S_6]^{4-}$ dimers first organize and undergo condensation–polymerization around the template to form a poorly registered, turbostratic layered arrangement. There is order only along the direction orthogonal to the tin sulfide sheets, with little order within and between the sheets. The final stage is associated with the registration of the tin sulfide sheets to give rise to a material with crystalline order over all three spatial dimensions. A schematic representation of this process is illustrated in Fig. 7.

Effect of temperature

It was surprising to discover that the framework of DABCOH-SnS-1 can be formed at room temperature and one atmosphere from a clear solution of the dimeric $[Sn_2S_6]^{4-}$ species, considering that microporous tin sulfides as well as microporous metal oxide materials, such as zeolites and aluminophosphates, are generally synthesized under hydrothermal reaction conditions at elevated temperatures and pressures.[27] This indicates that in the particular case of the formation of the SnS-*n* materials, the hydrothermal reaction conditions mainly serve to digest the source materials in the presence of mineralizers and is not essential for the formation of the microporous layered tin sulfide frameworks. For example, starting from a reaction mixture of Sn : 2 S : DABCO : 30 H_2O, unreacted sulfur and tin metal, as well as tin polysulfides were recovered if the reaction temperature was 100 °C or lower. Aging at room temperature generally enhances the passivation occurring on the tin surface.

The quality of hydrothermally grown crystals was found to

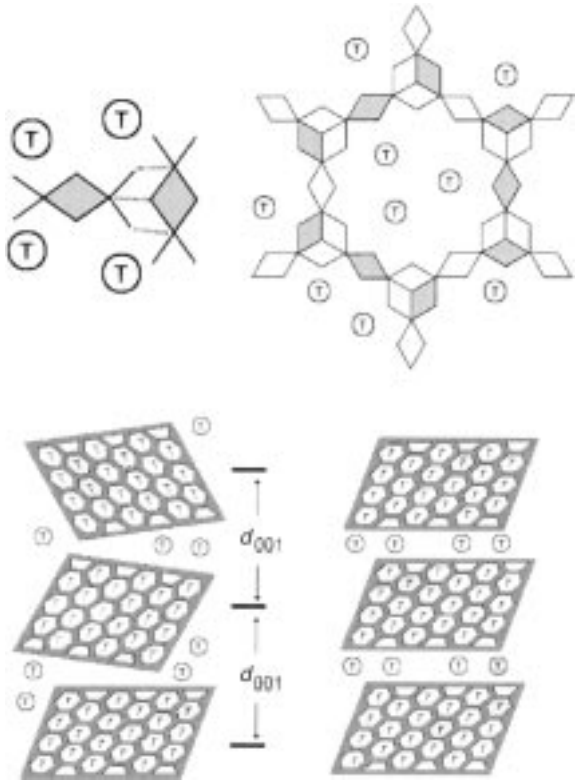

Fig. 7 A schematic representation of the self-assembly process of the dimer to the microporous layered structure of SnS-1

be sensitive to the rate of heating of the reaction mixture to the crystallization temperature and the rate of cooling it back to room temperature. Generally an initial slow rise of temperature reduces twinning or multicrystal growth and slow cooling gives crystals with cleaner surfaces and fewer small crystals. This implies that a fast rate of cooling generates supersaturation and new viable seed nuclei which only have a chance to grow for a short period of time, and therefore lead to smaller crystallites. In addition, secondary nucleation centres may grow on existing crystals. Crystals obtained from controlled slow cooling are generally larger than those from natural cooling as they consume the nutrients instead of creating secondary nuclei and small crystals.

Effect of mineralizers

By definition, in a hydrothermal synthesis mineralizers are the reagents that solubilize the source materials. In the hydrothermal synthesis of microporous tin sulfides, a mineralizer would be any chemical that can solubilize tin and sulfur. Hydroxide, fluoride, amine and sulfide have been employed as mineralizers in this study. Sulfide that reacts with sulfur to form soluble polysulfide under basic conditions was found to be an excellent mineralizer for sulfur. The solublility of polysulfides further accelerates the redox reaction between tin and sulfur. Sulfide also serves as an extra sulfur source required for the formation of the SnS-*n* materials. Hydroxide, fluoride and amine can solubilize elemental tin through a coordination reaction. If they are present in a large excess, all the available tin and sulfur may be present as strongly complexed soluble species and no solid SnS-*n* product forms. For example, a clear solution results from a reaction mixture of $2.5\,Et_4NOH : Sn : 2\,S : 30\,H_2O$ after a hydrothermal reaction at 150 °C over 3 days. Addition of NH_4F to the synthesis of TPA-SnS-3 significantly reduces the passivation of the tin surface and produces crystals with uniform size, indicating that crystal nucleation and growth processes occur over similar time periods.

Growth of large single crystals *vs.* synthesis of phase pure materials

It can be deduced from the above discussions that large single crystals of SnS-1 materials can be best produced in a static reactor by reducing the solubility of tin through lowering the concentration of mineralizers or utilizing those having weaker solubilizing ability toward tin. Slow heating and cooling generally favor high quality single crystals with cleaner surfaces. In contrast, for the preparation of phase pure materials, a small excess of mineralizers and agitation of the reaction mixture are necessary to bring all of the tin metal into product forming reactions. The redox reactions between tin and sulfur generates tin(IV) and sulfur(−II) in a ratio of 1 : 2, however, in SnS-1 and SnS-3 the ratio is 3 : 7 and 4 : 9, respectively. In order to prevent the formation of tin dioxide impurity, an extra sulfide source is necessary. Owing to the flexible framework properties and metastable nature of the SnS-*n* materials, products obtained from static and dynamic crystallization conditions may have entirely different structures. This makes the synthesis of a particular SnS-*n* structure, in both phase-pure and large single crystal forms, an interesting and challenging task.[19]

Conclusions

In the formation of microporous layered SnS-*n* materials, the dissolution and redox reactions of the elemental Sn and S sources are found to be extremely sensitive to the pH, concentration, mineralizers and reaction profile. Three types of reaction intermediates, $(CHA)_2Sn_2S_6$, $(AMTAH)_2S_2O_3$ and $(DABCOH)_2Sn(S_4)_3 : (DABCOH)_2Sn(S_4)_2(S_6)$ have been isolated and characterized through SCXRD structure analysis. A solution phase UV–VIS and ^{119}Sn NMR study of the mother-liquors of TEA-SnS-1 and TPA-SnS-3 synthesis systems all suggest that the dimeric $[Sn_2S_6]^{4-}$ species is the primary solution tin-containing species. It is interesting to recognize that the linkage of two $[Sn_2S_6]^{4-}$ building blocks in the configuration illustrated in Fig. 3A creates the Sn_3S_4 broken-cube clusters found in the SnS-*n* materials. Noteworthy is the discovery that DABCOH-SnS-1 can be formed from the condensation–polymerization of the dimeric $[Sn_2S_6]^{4-}$ species, in the presence of DABCO templates under ambient conditions, through precise control of pH. It should be feasible to build novel tin sulfide-based framework structures using other molecular building units, such as tetrameric $[Sn_4S_{10}]^{4-}$. The $[Ge_4S_{10}]^{4-}$ anion has already been successfully employed to build various gemanium sulfide-based 3D open frameworks.[4] A wide group of transition metals have also been incorporated into the gemanium sulfide-based frameworks where the transition metal is bonded to the terminal sulfurs of $[Ge_4S_{10}]^{4-}$ and serves to link together the $[Ge_4S_{10}]^{4-}$ building units.[4] Ternary metal tin sulfide open-frameworks are expected to emerge from the modular assembly of $[Sn_2S_6]^{4-}$ and $[Sn_4S_{10}]^{4-}$ building units with transition metal linkages. In addition, open framework materials built-up of mixed metal sulfides may be synthesized through the assembly of mixtures of molecular building blocks, for example $[Ge_4S_{10}]^{4-}$ and $[Sn_4S_{10}]^{4-}$. Introduction of other chalcogenides and metal chalcogenide clusters, such as $[In_2S_6]^{6-}$ and $[In_4S_{10}]^{8-}$, into the SnS-*n* structures, should modify their electrical and optical properties to produce interesting new classes of open framework metal chalcogenide materials.

Experimental

Materials preparation

$(CHAH)_4Sn_2S_6$ crystals. Single crystals of dimeric $(CHAH)_4Sn_2S_6$ were obtained from a reaction mixture of $1\,Sn : 2\,S : CHA : 35\,H_2O$. The cyclohexylamine was dissolved in deionized water, followed by addition of elemental S and

Sn powders. The resulting mixture was stirred vigorously at room temperature for 20 min and sealed in a Teflon® lined stainless autoclave and heated at 150 °C statically for 2 days. The autoclave was cooled down to room temperature at a rate of 8 °C h^{-1}. Needle-shaped transparent crystals of $(CHAH)_4Sn_2S_6$, a couple of mm in length, were recovered by filtration and washed with water and dried in air.

$(DABCOH)_2Sn(S_4)_3$ and $(DABCOH)_2Sn(S_4)_2(S)_6$ crystals. Red plate-shaped crystals of these two compounds were prepared from a reaction mixture of Sn : 2 S : DABCO : 37 H_2O. The DABCO was dissolved in water, followed by addition of S and Sn powders. The mixture was stirred vigorously at room temperature for 30 min and allowed to crystallize in a Teflon bottle at 100 °C over a period of 7 days. During the first 2 days, the Teflon bottle was shaken manually from time to time. Products were collected by filtration and washed with water.

Mother-liquors of TEA-SnS-1, TPA-SnS-3 and DABCOH-SnS-1. The TEA-SnS-1 and TPA-SnS-3 materials were obtained from a reaction mixture of Sn : 2 S : TEAOH : 30 H_2O and Sn : 2.25 S : TPAOH : 160 H_2O, respectively. The reaction mixtures were prepared following the same procedure as described above for $(CHAH)_4Sn_2S_6$ and were heated at 150 °C over 1–10 days, statically for TEA-SnS-1 and dynamically for TPA-SnS-3. The resulting mother-liquors were separated from the solid product by microfiltration and immediately used for ^{119}Sn NMR and UV–VIS measurements. The pH of the initial reaction mixture of the TPA-SnS-3 system was adjusted by addition of aqueous HCl for pH-dependent studies.

Studies of the mother-liquor of DABCOH-SnS-1 involved a reaction mixture of composition DABCO : Sn : 2 S : $(NH_4)_2S$: 30 H_2O. The DABCO was dissolved in deionized water and an aqueous solution of $(NH_4)_2S$ was then added. To this solution, elemental S and Sn were added and stirred well until all the sulfur had dissolved. The reaction mixture was allowed to crystallize dynamically in a Teflon lined stainless steel autoclave at 150 °C for 3 h. The resulting mother-liquor was filtered through a fritted glass disk under N_2 and stored in an inert atmosphere. Bubbling of CO_2 through the mother-liquor was performed using a vacuum line. For the study of the effect of concentration of DABCO on the crystal size of DABCOH-SnS-1, the starting reaction mixture used was x DABCO : 2 $(NH_4)_2S$: 60 H_2O : 2 S : Sn with x varying between 0.2 and 2.5, and crystallized statically at 150 °C for 2 days.

Physical measurements

The mother-liquors were used directly for ^{119}Sn NMR data collection after the solid products had been removed by filtration. The ^{119}Sn NMR spectra were recorded at 111.817 MHz on a Varian Gemini 300 MHz broadband spectrometer, locked to D_2O in a coaxial 10 mm tube. The chemical shift of the ^{119}Sn NMR signal was referenced against an external standard Me_4Sn. Solution UV–VIS absorption spectra were obtained on a Hewlett Packard 8452A diode array spectrometer. The mother-liquor was diluted with a dilute aqueous solution of Et_4NOH, or $Pr^n{}_4NOH$, or DABCO with the same pH as that of the mother-liquor. To determine the absorption coefficient of $(CHAH)_4Sn_2S_6$, known amounts were dissolved in deionized water. The pH-dependence study was conducted by dissolving $(CHAH)_4Sn_2S_6$ crystals in aqueous solutions of HCl or NaOH at various concentrations. Powder XRD patterns were collected on a Siemens D5000 diffractometer with Cu-Kα radiation. Single crystal XRD data were recorded using Enraf-Nonius CAD4 and Siemens P4 diffractometers. Scanning electron micrograph (SEM) images were recorded on a Hitachi S-570 microscope with an accelerating voltage of 20 kV.

X-Ray structural characterization

A summary of selected crystallographic data is given in Table 1. Data for all compounds were collected using graphite monochromated Mo-Kα radiation ($\lambda = 0.710\,73$ Å). The structures were solved and refined using the SHELXTL/PC[ref1] package.[28] Refinement was by full-matrix least-squares on F^2 using all data (negative intensities included). For each compound the non-hydrogen atoms were refined with anisotropic thermal parameters and the hydrogen atoms were included in calculated positions and treated as riding atoms. In the structures of **2** and **3** $wR2 = 0.3979$ and 0.3868, respectively. For these particular structure determinations the origin of the high $wR2$ values most likely arises from the fact that the crystals were both weak diffractors and were of high mosaicity. Weak reflections which were measured with high statistical error were rejected from the least-squares refinement but were included in the final calculation of $wR2$. Furthermore in the case of **2** the structure is also disordered. The disordered polysulfide fits a chemically and structurally reasonable model but slight imperfections in the constrained model will contribute to a higher value of $wR2$. The slightly higher U_{eq} of S(5) in structure **2** arises because this sulfur atom is in the region of the disordered polysulfide ligand. Full crystallographic details, excluding structure factors, have been deposited at the Cambridge Crystallographic Data Centre (CCDC). See Information for Authors, *J. Mater. Chem.*, 1998, Issue 1. Any request to the CCDC for this material should quote the full literature citation and the reference number 1145/78.

The generous financial assistance of the Natural Sciences and Engineering Research Council of Canada, the Canadian Space Agency (CSA) and Universal Oil Products (UOP) is deeply appreciated. T. J. expresses her gratitude to the University of Toronto for a graduate scholarship held during the course of this work. The technical assistance of Dr Srebri Petrov for the quantitative PXRD analysis, Mr Nick Palvac for solution NMR data collection, and Dr Neil Coombs for SEM images proved to be most valuable. Special thanks go to all the G.A.O. team members that participated in the study of the self-assembly of microporous layered tin sulfides.

References

1 (*a*) T. Jiang, A. L. Lough, G. A. Ozin, D. Young and R. L. Bedard, *Chem. Mater.*, 1995, **7**, 245; (*b*) H. Ahari, C. L. Bowes, T. Jiang, A. L. Lough, G. A. Ozin, R. L. Bedard, S. Petrov and D. Young, *Adv. Mater.*, 1995, **7**, 375; (*c*) T. Jiang, Ph. D. Thesis, University of Toronto, 1997.

2 R. E. Melendez, C. V. K. Sharma, M. J. Zaworotko, C. Bauer and R. D. Rogers, *Angew. Chem., Int. Ed. Engl.*, 1996, **35**, 2213.

3 J. Gopalakrishanan, *Chem. Mater.*, 1995, **7**, 1267.

4 C. L. Bowes, W. U. Huynh, S. J. Kirkby, A. Malek, G. A. Ozin, S. Petrov, M. Twardowski, D. Young, R. L. Bedard and R. Broach, *Chem. Mater.*, 1996, **8**, 2147; C. L. Bowes, A. J. Lough, S. J. Kirkby, G. A. Ozin, S. Petrov, M. Twardowski and D. Young, *Chem. Ber.*, 1996, **129**, 283; A. Loose and W. S. Sheldrick, *Verlag der Zeitschrift fur Naturforschung*, 1997, 687 and references cited therein.

5 T. Jiang, G. A. Ozin and R. L. Bedard, *Adv. Mater.*, in press; *Adv. Mater.*, 1994, **6**, 860.

6 (*a*) C. Brevard and P. Granger, *Handbook of High Resolution Multinuclear NMR*, John Wiley & Sons, New York, 1981; (*b*) J. Emsley, *The Elements*, Oxford University Press, 1991; (*c*) P. G. Harrison, in *Chemistry of Tin*, Blackie, Glasgow, 1989; (*d*) J. Mason, *Multinuclear NMR*, Plenum, New York, 1987; (*e*) I. D. Gay, C. H. Jones and C. V. K. Sharma, *J. Magn. Reson.*, 1989, **84**, 501.

7 C. Mundus, G. Taillades, A. Pradel and M. Ribes, *Solid State Nucl. Magn. Reson.*, 1996, **7**, 141.

8 D. Dakternieks H. Zhu, D. Masi and C. Mealli, *Inorg. Chem*., 1992, **31**, 3601; K. B. Dillon, A. Marshall, *J. Chem. Soc., Dalton Trans*., 1984, 1245.
9 D. Young, unpublished work, personal communication.
10 W. S. Sheldrick, personal communication.
11 B. Krebs, *Angew. Chem. Int. Ed. Engl*., 1983, **22**, 113.
12 H. Schumann, *Reaction of Elemental Sulfur with Inorganic, Organic and Metal Organic Compounds*, in *Sulfur in Organic and Inorganic Chemistry*, ed. A. Senning, Marcel Dekker, Inc., New York, 1972.
13 P. P. Paul, T. B. Rauchfuss and S. R. Wilson, *J. Am. Chem. Soc*., 1993, **115**, 3316; E. Ramli, T. B. Rauchfuss and C. L. Stern, *J. Am. Chem. Soc*., 1990, **112**, 4043.
14 D. Dev, E. Ramli, T. B. Rauchfuss and S. R. Wilson, *Inorg. Chem*., 1991, **30**, 2514.
15 A. K. Verma, T. B. Rauchfuss and S. R. Wilson, *Inorg. Chem*., 1995, **34**, 3316.
16 (*a*) S. Licht, *J. Electrochem. Soc*., 1987, **134**, 2137, 1988, **135**, 2971; (*b*) W. F. Giggenbach, *Inorg. Chem*., 1974, **13**, 1724.
17 A. Müller, J. Schimanski, M. Römer, H. Bögge, W. Baumann, W. Eltzner, E. Krickemeyer and U. Billerbeck, *Chimia*, 1985, **39**, 25.
18 L. Cambi, *US Pat*., 3 427 126, 1963.
19 H. Ahari, C. L. Bowes, N. Coombs, Ö. Dag, T. Jiang, A. Lough, G. A. Ozin, S. Petrov, I. Sokolov, A. K. Verma, G. Vovk and D. Young, *Microgravity Sci*., February, 1997; H. Ahari, R. L. Bedard, C. L. Bowes, N. Coombs, Ö. Dag, T. Jiang, A. Lough, G. A. Ozin, S. Petrov, I. Sokolov, A. K. Verma, G. Vovk and D. Young, *Nature (London)* 1997, **388**, 857; Ö. Dag, H. Ahari, N. Coombs, T. Jiang, P. Aroca-Ouellette, S. Petrov, I. Sokolov, A. K. Verma, G. Vovk, D. Young, R. L. Bedard and G. A. Ozin, *Adv. Mater*., 1979, **9**, 1133.
20 (*a*) B. M. Lok, T. R. Cannan and C. A. Messina, *Zeolites*, 1983, **3**, 282; (*b*) D. W. Lewis, C. R. Catlow and J. M. Thomas, *Chem. Mater*., 1996, **8**, 1112; (*c*) D. W. Lewis, C. M. Freeman and C. R. A. Catlow, *J. Phys. Chem*., 1995, **99**, 11 194; (*d*) C. J. Brinker, *Curr. Opin. Solid State Mater. Sci*., 1996, **1**, 798; (*e*) R. F. Lobo, S. I. Zones and M. E. Davis, *J. Inclusion Phenom. Mol. Recognit*., 1995, **21**, 47.
21 S. L. Burkett and M. E. Davis, in *Advances in Porous Materials*, ed. S. Komarneni, D. M. Smith and J. S. Beck, Materials Research Society, Pittsburgh, 1995, p. 3.
22 S. L. Burkett and M. E. Davis, *J. Phys. Chem*., 1994, **98**, 4647.
23 G. A. Marking and M. G. Kanatzidis, *Chem. Mater*., 1995, **7**, 1915.
24 C. L. Bowes, PhD Thesis, University of Toronto, 1996.
25 W. S. and H.-G. Braunbeck, *Z. Naturforsch. Teil B*, 1990, **45**, 1643.
26 R. J. Francis, S. J. Price, J. S. O. Evans, S. O'Brien and D. O'Hare, *Chem. Mater*., 1996, **8**, 2102.
27 R. M. Barrer, *Hydrothermal Chemistry of Zeolites*, Academic Press, London, 1982.
28 G. M. Sheldrick, SHELXTL/PC, Siemens Analytical X-ray Instruments Inc., Madison, WI, 1994.

Paper 7/06042D; *Received* 18*th August*, 1997